Face-Centered-Cubic Lithium Crystals Formed in Mesopores of Carbon Nanofiber Electrodes

Byoung-Sun Lee,[†] Jong-Hyun Seo,[‡] Seoung-Bum Son,[†,§] Seul Cham Kim,[†] In-Suk Choi,[⊥] Jae-Pyoung Ahn,[‡] Kyu Hwan Oh,[†] Se-Hee Lee,[§] and Woong-Ryeol Yu[†,*]

[†]Department of Materials Science and Engineering and Research Institute of Advanced Materials, Seoul National University, 1 Gwanak-ro, Gwanak-gu, Seoul 151-742, Republic of Korea, [‡]Advanced Analysis Center, Korea Institute of Science and Technology, Seoul 136-791, Republic of Korea, [§]Department of Mechanical Engineering, University of Colorado, 427 UCB, Boulder, Colorado 80309, United States, and [⊥]High Temperature Energy Center, Korea Institute of Science and Technology, Seoul 136-791, Republic of Korea

ABSTRACT In the foreseeable future, there will be a sharp increase in the demand for flexible Li-ion batteries. One of the most important components of such batteries will be a freestanding electrode, because the traditional electrodes are easily damaged by repeated deformations. The mechanical sustainability of carbon-based freestanding electrodes subjected to repeated electrochemical reactions with Li ions is investigated *via* nanotensile tests of individual hollow carbon nanofibers (HCNFs). Surprisingly, the mechanical properties of such electrodes are improved by repeated electrochemical reactions with Li ions, which is contrary to the conventional wisdom that the mechanical sustainability of carbon-based electrodes should be degraded by repeated electrochemical reactions. Microscopic studies reveal a reinforcing mechanism behind this improvement, namely, that inserted Li ions form irreversible face-centered-cubic (FCC) crystals within HCNF cavities, which can reinforce the carbonaceous matrix as strong second-phase particles. These FCC Li crystals formed within the carbon matrix create tremendous potential for HCNFs as freestanding electrodes for flexible batteries, but they also contribute to the irreversible (and thus low) capacity of HCNFs.

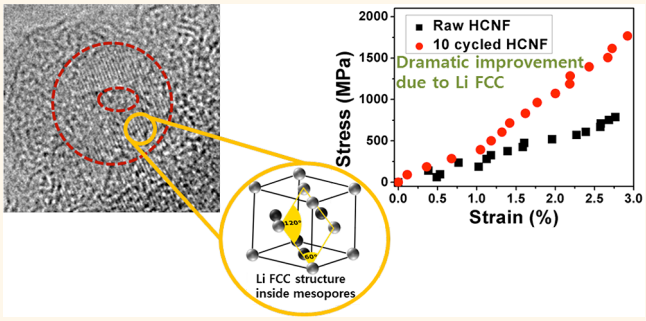

KEYWORDS: hollow carbon nanofibers · flexible Li-ion battery · freestanding electrode · irreversible capacity · Li FCC crystal

Since the early 1990s, Li-ion batteries have been widely used as the main power source for small, portable electronic devices, such as mobile phones, mp3 players, laptops, and others.[1] As visionary and creative new portable devices (*e.g.*, wearable electronic devices for the military, healthcare, and space exploration,[2] smart-textile-based electronic systems,[3,4] and deformable electronics such as roll-up displays, stretchable circuits, and electronic paper[5]) continue to be introduced, a strong demand is created for the innovative development of flexible Li-ion batteries. Traditional Li-ion battery systems employing lithium metal oxide cathodes and graphite anodes cannot be directly utilized as flexible batteries, because they are easily pulverized by a small external load. Accordingly, a large amount of research has been directed toward the development of tough, deformable electrodes.

In the context of a flexible battery, the term "freestanding electrode" often refers to a type of tough, deformable electrode for which carbon nanomaterials, such as carbon nanotubes (CNTs) and graphenes, can be regarded as satisfactory candidates due to their excellent mechanical properties and stable electrochemical behavior.[6−9] However, the low specific capacity of carbon (372 mAh g^{-1}) is an obstacle to the realization of freestanding CNT or graphene electrodes. Composite electrodes, combining these materials with electrochemically excellent materials such as Si, SnO_2, V_2O_5, Ge, and others, have been researched;[10−14] it is important to ensure the mechanical sustainability of carbon nanomaterials after electrochemical reactions. Nevertheless, there

* Address correspondence to woongryu@snu.ac.kr.

Received for review February 11, 2013 and accepted June 3, 2013.

Published online June 03, 2013
10.1021/nn4019625

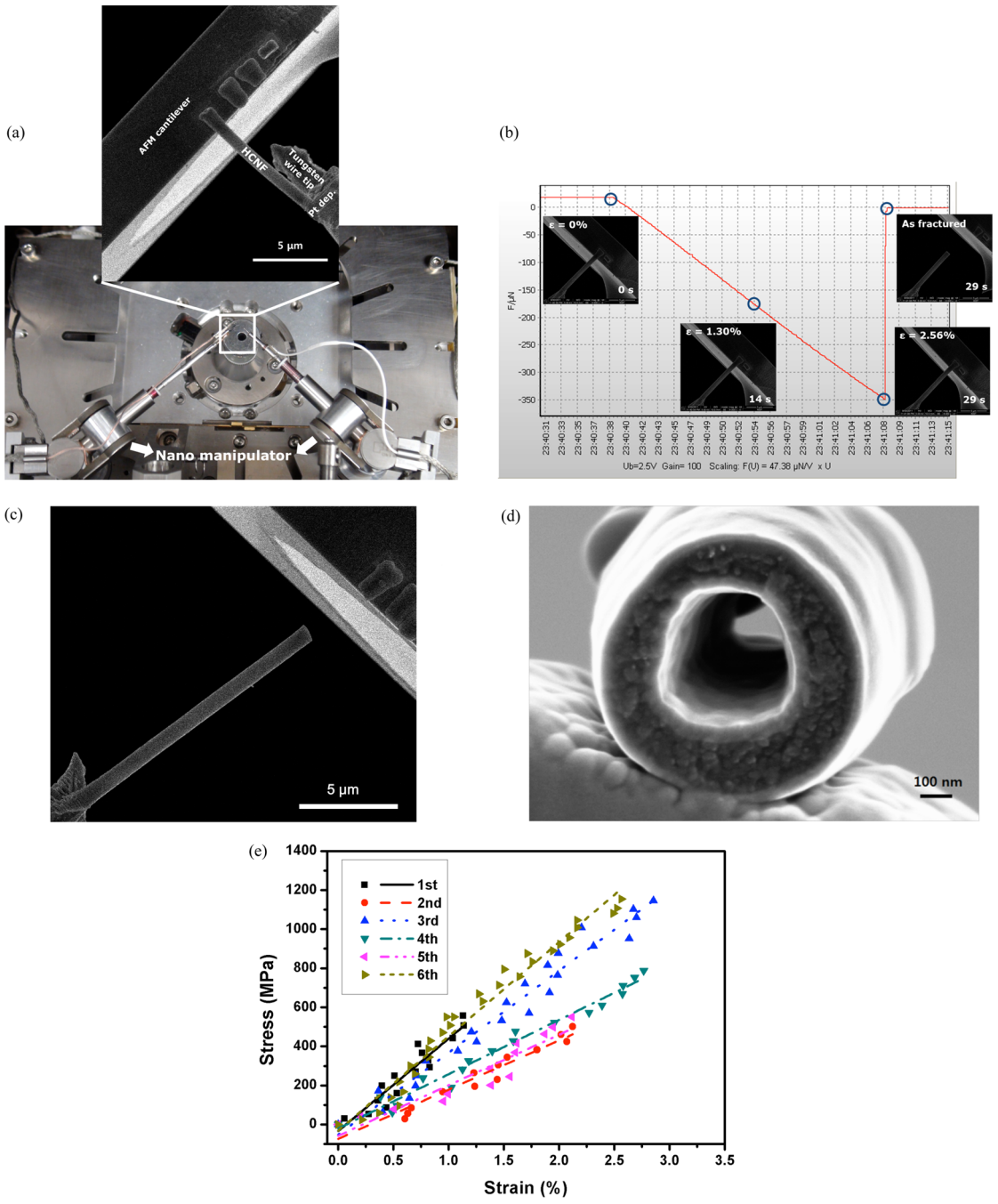

Figure 1. (a) Nanotensile test setup in an FIB instrument. One end of a single HCNF filament is attached to the end of a tungsten wire tip, while the other end is attached to an FMT cantilever. The nanomanipulator pulls the tungsten wire, deflecting the FMT cantilever. (b) Real-time monitoring of nanotensile testing. The strain is recorded by field-emission (FE)-SEM, while the force is measured in real time. The strain and stress are synchronized from the recorded time sequence. (c) SEM image of fractured HCNFs. Most HCNF fractures due to tensile load occurred around the FMT cantilever, indicating a lack of critical defects within the gauge region. (d) SEM image of a fractured surface, enabling a precise calculation of the stress. (e) Stress–strain curves of individual HCNFs.

has been little research on this issue, although the mechanical properties of pristine CNTs or graphenes have been investigated.[15,16] As a consequence, the feasibility of carbon nanomaterials for freestanding electrodes remains unknown.[4,6,17]

On the other hand, poly(acrylonitrile) (PAN)-based carbon nanofibers (CNFs), manufactured by electrospinning and a subsequent thermal treatment, are potential candidates for freestanding electrodes due to their mechanical stability, convenient processing, and scalability for mass production.[18,19] In particular, hollow carbon nanofibers (HCNFs)[20−24] are among the most satisfactory carbon nanomaterials, because the low capacity of carbon can easily be enhanced by encapsulating Si, Sn, or S into their hollow cores. The buffering effect (and thus the enhanced capacity) of

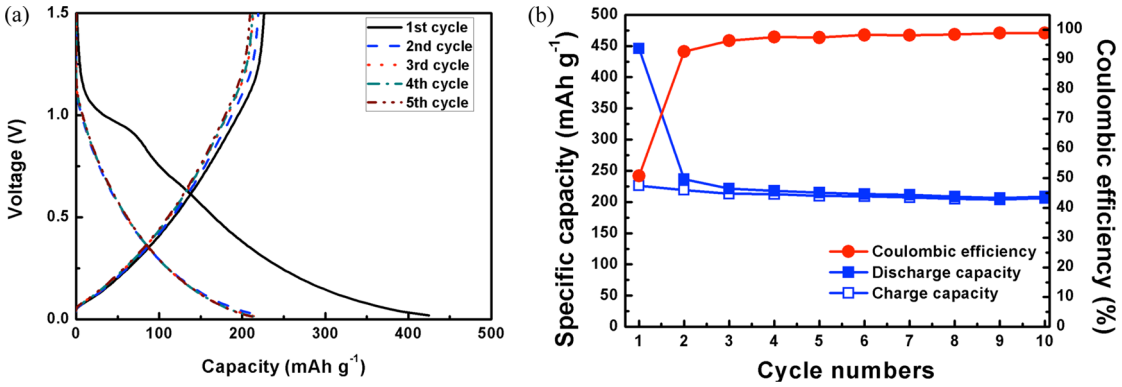

Figure 2. (a) Voltage profiles during the first five lithiation and delithiation cycles. The inflection is more significant around 0.85 V than it is around 0.75 V, implying that lithium insertion is facilitated by the lack of a binder polymer and acetylene black. (b) Cycling performances of freestanding HCNF anodes. The rapid convergence of the specific capacity is similar to that observed in the authors' previous work.[21]

HCNFs has been observed by the *in situ* lithiation of Si core/C shell nanofibers.[22] However, the mechanical sustainability of HCNFs during electrochemical reactions has not yet been investigated. In this work, the mechanical sustainability of freestanding HCNF anodes subjected to repeated electrochemical reactions was investigated *via* nanotensile tests of individual HCNFs. The microstructural changes incurred during the electrochemical reactions were carefully studied to relate the mechanical properties of HCNFs with their microstructures and evaluate their potential use as freestanding electrodes.

RESULTS AND DISCUSSION

***In Situ* Nanotensile Test.** HCNFs were prepared by the coaxial electrospinning of styrene-*co*-acrylonitrile (SAN) core/PAN shell solutions and a subsequent thermal treatment (Figure S1).[20] The detailed processing conditions and the microstructures of the HCNFs are discussed in the Methods section. The mechanical properties of the HCNFs were characterized by a nanotensile test in a focused ion beam (FIB) instrument. First, a single HCNF was attached to the tip of a tungsten wire using a nanomanipulator (Kleindiek) and Pt deposition. The opposite end of the HCNF was fixed to the end of a force-measurement tip (FMT) cantilever (FMT-120, Kleindiek) *via* Pt deposition (Figure 1(a)). As the nanomanipulator and tungsten wire pulled the HCNF along its fiber axis, the force acting on the HCNF was measured. The force on the HCNF was recorded *in situ*, while the strain was calculated using discrete and sequential scanning electron microscopy (SEM) images (see Figure 1(b)). Detailed procedures for this test including the calibration and the sensitivity of measured force are provided in the Supporting Information. The complete nanotensile test procedure is recorded in Movie S1. The HCNFs were fractured near the FMT cantilever, most likely due to the stress concentration in that area (Figure 1(c)), implying a uniform HCNF microstructure without critical defects within the gauge region.[25] The cross-sectional area of the fractured HCNF was measured using an SEM image (Figure 1(d)), making it possible to calculate the stress. Finally, the complete stress−strain curve of an individual HCNF was obtained (Figure 1(e)). Note that this curve is virtually linear; the average Young's modulus and HCNF strength are 30.4 GPa (±8.6 GPa) and 0.76 GPa (±0.30 GPa), respectively. The average breaking strain of the HCNFs is 2.49% (±0.49%). The HCNF modulus and strength are lower than those of solid CNFs,[25,26] while the breaking strain is greater than that of solid CNFs,[25,26] due to the porous nature and microstructure of the HCNFs. A detailed discussion, including a discussion of the HCNF fracture mechanism, is provided in the Supporting Information.

Electrochemical Reactions and Mechanical Properties. The electrochemical performance of freestanding HCNF anodes was first characterized at a current density of 50 mA g^{-1} (see the Supporting Information for the detailed experimental procedure). Typical voltage profiles during the first five cycles are shown in Figure 2(a). The inflection is more significant around 0.85 V (lithium insertion into the cavities[27]) than it is around 0.75 V (solid electrolyte interface formation[23]) on the first discharge curve. This occurs due to the relatively easy insertion of Li ions into the freestanding HCNFs due to the lack of binder polymers or carbon black. Reversible intercalation is also confirmed by the inflection below 0.2 V.[21,23] From the cycling performance curve (Figure 2(b)), the calculated values of the reversible and initial irreversible capacities are 226 mAh g^{-1} and 47%, respectively. The reversible capacity of the freestanding HCNFs decreased to 62.5%, while their initial irreversible capacity increased slightly, compared to the nonfreestanding HCNF anodes in the authors' previous work.[23] The reversible capacity of the freestanding HCNFs converged to 206 mAh g^{-1} after 10 cycles.

Some of the HCNFs were taken from the electrode after the first lithiation and delithiation processes, and their mechanical properties were characterized using the nanotensile test. The mechanical properties of

HCNFs that underwent 10 electrochemical reaction cycles were also measured. Note that the maximum number of electrochemical cycles was fixed at 10 because the freestanding HCNF anodes exhibited convergent cycling behavior within 10 cycles.[23] Astonishingly, the mechanical performance of the HCNFs improved after undergoing the electrochemical reactions, as shown in Table 1. These results are contradictory to the conventional wisdom that inserted Li ions alter the crystalline structure of carbonaceous materials (including HCNFs), resulting in degraded mechanical properties.[28] The electrochemically reacted HCNFs exhibited nonlinear stress–strain behavior, as shown in Figure 3, implying that the electrochemical reactions bring about microstructural changes in the HCNFs. The nonlinear behavior (*viz.*, the slope changes in the stress–strain curves) indicates that the deformation mode changed as the stress increased, which is often observed in particulate composite materials.[29]

TABLE 1. Mechanical Properties and Microstructures of HCNFs According to the Number of Electrochemical Reaction Cycles[a]

sample	strength (GPa)	strain (%)	modulus (GPa)	d_{002} (nm)	$D_{Li\ FCC}$ (nm)
raw HCNF	0.76(0.30)	2.49(0.49)	30.4(8.6)	0.352	
1st lithiated HCNF	1.06(0.56)	2.78(0.38)	36.7(13.9)	0.389	2.94(0.71)
1st delithiated HCNF	1.32(0.30)	2.68(0.28)	49.5(11.7)	0.372	4.20(0.69)
10-cycled HCNF	1.67(0.15)	2.67(0.59)	63.9(9.7)	0.366	4.54(0.82)

[a] The numbers in parentheses represent the standard deviation of the values.

Faced-Centered-Cubic Lithium Crystals. The microstructure of the electrochemically reacted HCNFs was investigated to identify the microstructural changes that occurred during the reaction. Well-developed donut-shaped crystallites were observed in both lithiated and delithiated HCNFs (see Figure 4(a,b)), implying that the crystallites filled the mesopores ($D \approx 8.33$ nm[23]) of the HCNFs. Because vacant regions were filled with solid crystallites, the HCNFs became more rigid; that is, the crystallites acted as second-phase rigid particles in particulate composite materials (Figure 4(c)). Because the tensile strength of the HCNFs increased, the adhesion (interfacial bonding) between the crystallites and carbons in the HCNFs was quite strong, contributing to the number of leftover crystallites after delithiation. The atomic composition of the HCNFs and the electrochemical reactions indicate that the crystallites were lithium compounds. The interlayer spacing of the crystallites in both the lithiated and delithiated HCNFs was characterized as 0.2 nm based on the high-resolution transmission electron microscopy (HR-TEM) images in Figure 4(a,b). Crystallites with the same interlayer spacing were observed in a previous study,[30] in which they were hypothesized to be face-centered-cubic (FCC) Li crystals without decisive evidence.

The interlayer distances between the crystalline layers were found to be 0.237, 0.207, 0.147, 0.127, 0.119,

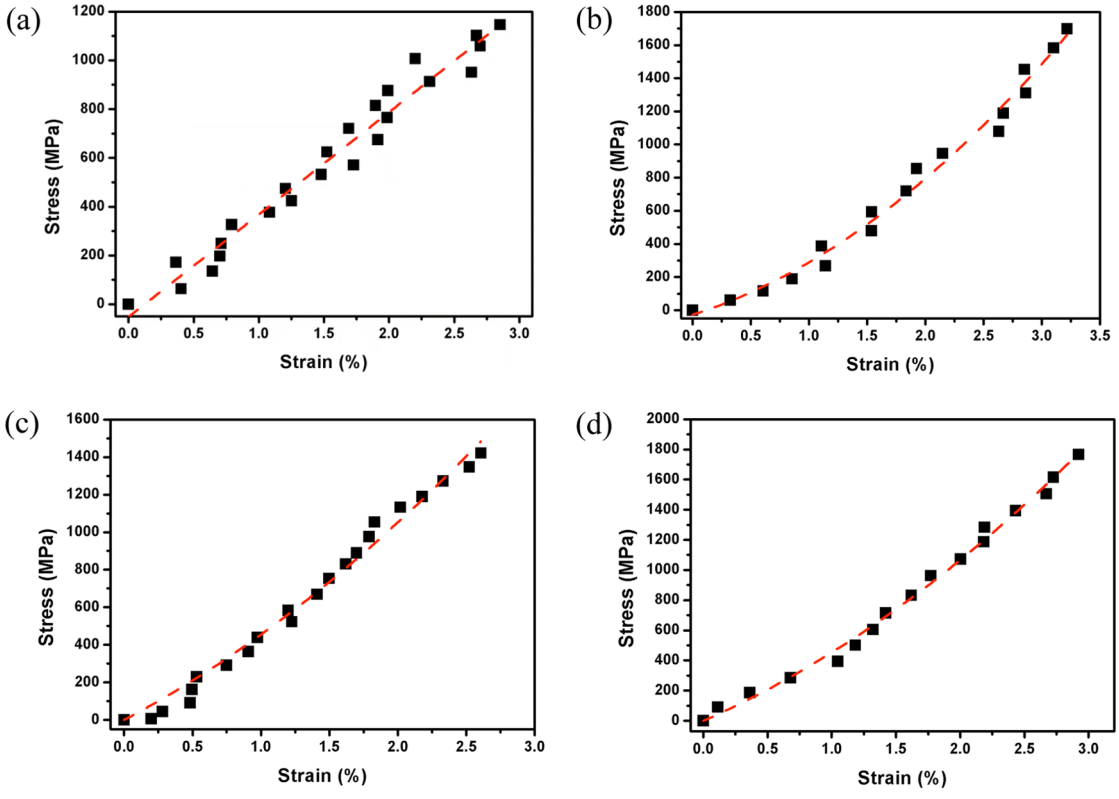

Figure 3. Typical stress–strain curves of (a) raw, (b) first lithiated, (c) first delithiated, and (d) 10-cycled HCNFs. Unlike the tensile behavior of the raw HCNFs, the stress–strain curves of the electrochemically reacted HCNFs are nonlinear.

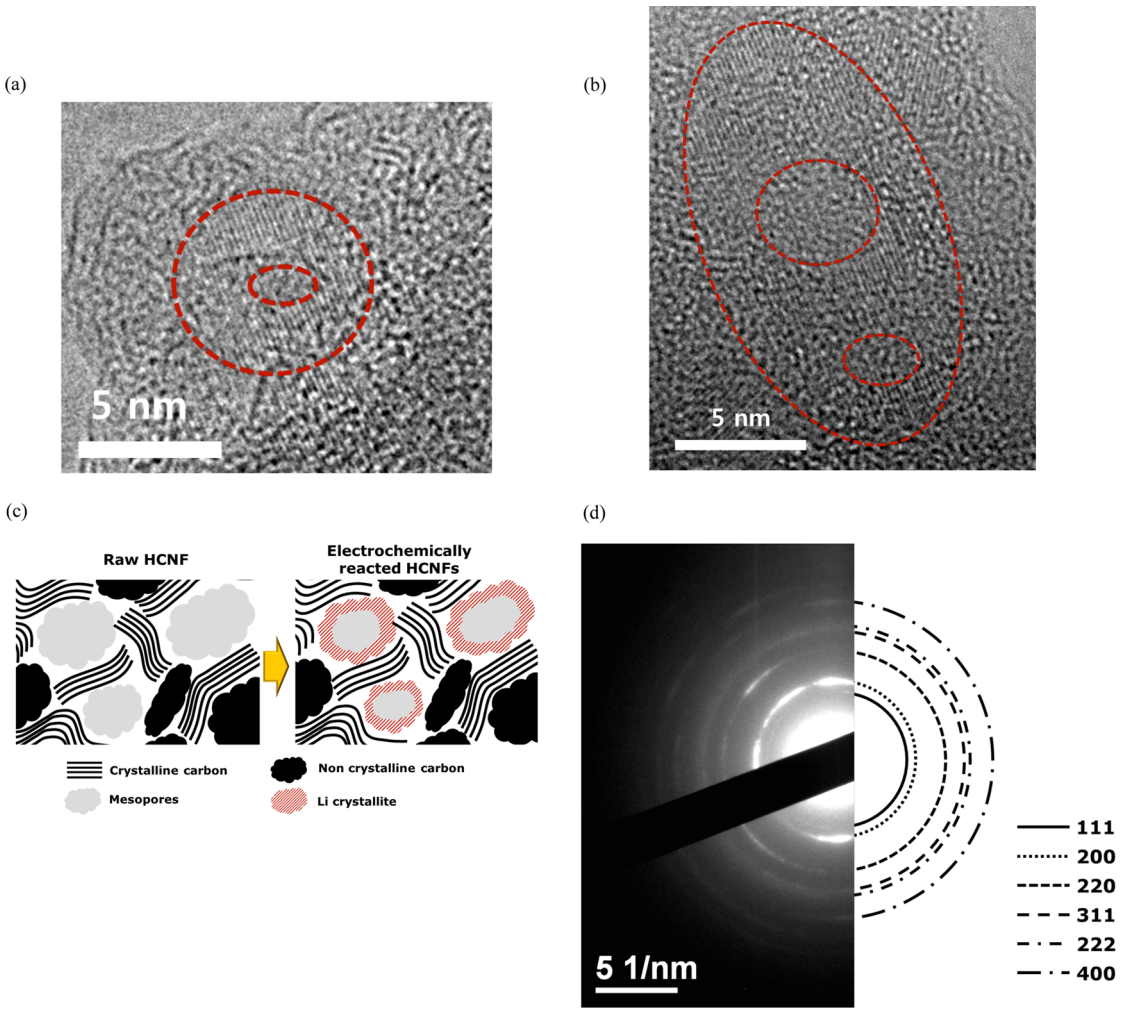

Figure 4. Crystalline microstructure formed after the electrochemical reaction. HR-TEM images of donut-shaped lithium FCC metal crystallites of the (a) first lithiated and (b) first delithiated HCNFs. (c) Schematic illustration of the microstructures of raw and electrochemically reacted HCNFs. (d) SAED pattern of the first lithiated HCNF.

and 0.104 nm, based on the selected area electron diffraction (SAED) pattern shown in Figure 4(d). These values do not match the JCPDS cards for LiC_6, Li_2O, Li_3N, LiH, or even Li body-centered-cubic (BCC) crystals. However, the calculated value of the lattice parameter (a_0) of a Li FCC crystal is 0.410 nm, based on the atomic radius of Li (0.145 nm).[31] Using this value, the interlayer distances can also be calculated: d_{111} = 0.237 nm, d_{200} = 0.205 nm, d_{220} = 0.145 nm, d_{311} = 0.124 nm, d_{222} = 0.118 nm, and d_{400} = 0.103 nm. These values match those obtained from the SAED pattern precisely, leading to the conclusion that FCC Li crystals formed in the freestanding HCNFs. Because the crystal structure of a Li electrode is commonly BCC, it is quite interesting to observe the formation of FCC Li crystals in porous carbon electrodes during electrochemical reactions with Li ions. At the moment, the origin of the FCC Li crystals is unknown and is beyond the scope of this research. Nevertheless, it can be inferred that the intercalated, rhombically arranged Li atoms in the graphitic carbon layers[32] protruded into the mesopores and acted as a seed layer for the FCC Li crystals; that is, the deionized Li ions were arranged into FCC crystals to maintain the coherency of the Li atomic arrangement (LiC_6) (see Figure S9 for a schematic illustration). This type of FCC crystal structure could explain the irreversible capacity observed in porous carbon electrodes. In general, the ionization energy of an FCC crystal is larger than that of a BCC crystal, owing to its structural stability,[33] and thus, FCC Li crystals that form in mesoporous carbon electrodes cannot be ionized over the range of electrical potentials (0.01 to 1.5 V) that ionize BCC Li crystals. Therefore, FCC Li crystals are partly responsible for the irreversible capacity of porous carbon electrodes in Li-ion batteries.

The size of the FCC Li crystals increased with the number of electrochemical reaction cycles: 2.94 nm (±0.71 nm) after the first lithiation process, 4.20 nm (±0.69 nm) after the first delithiation process, and 4.54 nm (±0.82 nm) after 10 cycles. These changes in size confirm the formation of irreversible (and also accumulated) Li crystals within the HCNFs and also their increasing contribution to the mechanical properties of

the HCNFs as the electrochemical reaction cycles proceeded. At the same time, the interlayer spacing between the turbostratic carbon layers in the HCNFs increased to 0.389 nm after the first lithiation process, which is comparable to that of pristine HCNFs (d_{002} = 0.352 nm). The expansion rate (10.5%) due to Li-ion intercalation is comparable to values commonly observed in carbonaceous materials.[34] The interlayer spacing was not fully recovered upon delithiation, although it decreased to 0.372 nm after the first delithiation step and to 0.366 nm after 10 cycles due to Li-ion deintercalation from the turbostratic interlayers, which also contributed to the irreversible lithium intercalation. The expanded turbostratic carbon layers along with the FCC Li crystals caused nonlinear stress–strain behavior of the electrochemically reacted HCNFs. In short, due to the microstructural changes driven during the electrochemical reaction, the modulus and strength of HCNFs are considerably improved, while their breaking strains are slightly increased. The evaluation and understandings of such improved mechanical properties will promote various research into the design of novel nanostructured electrodes using HCNFs for flexible, stretchable, and wearable Li-ion batteries.[35,36]

CONCLUSIONS

FCC Li crystals form in porous carbon electrodes, such as HCNFs, during electrochemical reactions with Li ions. The FCC Li crystals remain after delithiation because their ionization potential is higher than that of BCC Li crystals in a positive electrode. Thus, they are a main cause of the irreversible lithium intercalation and low capacity of porous carbon electrodes. On the other hand, the FCC Li crystals act as second-phase rigid particles, reinforcing the carbonaceous matrix and providing improved tensile properties to freestanding HCNFs undergoing electrochemical reactions. This mechanical role of FCC Li crystals is highly significant, as it enables mechanically sustainable freestanding electrodes to be realized using porous carbon nanomaterials.

METHODS

Preparation of HCNFs. Poly(acrylonitrile) (M_w = 200 000 g/mol, Misui Chemical) and styrene-*co*-acrylonitrile (M_w = 120 000 g/mol, AN = 28.5 mol %, Cheil Industries) were used as the carbonizing shell precursor and sacrificial core material, respectively. *N,N*-Dimethylformamide (99.5%) was used as the solvent for both the shell and core materials. The concentrations of PAN and SAN were 20 and 30 wt %, respectively. A coaxial nozzle with two concentric needles was designed to have gauge numbers of 17 and 22 for the shell and core, respectively. The setup for the coaxial electrospinning process was as follows: the applied voltage was 18 kV, the tip-to-collector distance was 15 cm, and the flow rates of the inner and outer solutions were 0.5 and 1 mL/h, respectively. The SAN core/PAN shell precursor nanofibers were thermally treated for stabilization (at 270–300 °C for 1 h in an air atmosphere) and carbonization (at 1000 °C for 1 h in an N_2 atmosphere) of the PAN shell. The ramping rates were set at 10 °C/min.

Conflict of Interest: The authors declare no competing financial interest.

Supporting Information Available: The microstructural analysis and electrochemical characterization of raw hollow carbon nanofibers (HCNFs) and the mechanical properties of individual HCNFs are discussed in a detailed manner, and supplementary figures and a movie are provided. This information is available free of charge *via* the Internet at http://pubs.acs.org.

Acknowledgment. This research was supported by Basic Science Research Program (2010-0022633), Engineering Research Center of Excellence Program (R11-2005-065), and Global Research Lab Program (2010-00351) through the National Research Foundation of Korea (NRF) funded by the Ministry of Education, Science and Technology (MEST). This research was also supported by a grant from the Fundamental R&D Program for Technology of World Premier Materials funded by the Ministry of Knowledge Economy, Republic of Korea (10037919).

REFERENCES AND NOTES

1. Endo, M.; Kim, C.; Nishimura, K.; Fujino, T.; Miyashita, K. Recent Development of Carbon Materials for Li Ion Batteries. *Carbon* **2000**, *38*, 183–197.
2. Park, S.; Jayaraman, S. Smart Textiles: Wearable Electronic Systems. *MRS Bull.* **2003**, *28*, 585–591.
3. Wang, C.; Li, D.; Too, C. O.; Wallace, G. G. Electrochemical Properties of Graphene Paper Electrodes Used in Lithium Batteries. *Chem. Mater.* **2009**, *21*, 2604–2606.
4. Wang, J.-Z.; Zhong, C.; Chou, S.-L.; Liu, H.-K. Flexible Free-Standing Graphene-Silicon Composite Film for Lithium-Ion Batteries. *Electrochem. Commun.* **2010**, *12*, 1467–1470.
5. Wang, D.-W.; Li, F.; Zhao, J.; Ren, W.; Chen, Z.-G.; Tan, J.; Wu, Z.-S.; Gentle, I.; Lu, G. Q.; Cheng, H.-M. Fabrication of Graphene/Polyaniline Composite Paper *via in Situ* Anodic Electropolymerization for High-Performance Flexible Electrode. *ACS Nano* **2009**, *3*, 1745–1752.
6. Chew, S. Y.; Ng, S. H.; Wang, J.; Novák, P.; Krumeich, F.; Chou, S. L.; Chen, J.; Liu, H. K. Flexible Free-Standing Carbon Nanotube Films for Model Lithium-Ion Batteries. *Carbon* **2009**, *47*, 2976–2983.
7. Ng, S. H.; Wang, J.; Guo, Z. P.; Chen, J.; Wang, G. X.; Liu, H. K. Single Wall Carbon Nanotube Paper as Anode for Lithium-Ion Battery. *Electrochim. Acta* **2005**, *51*, 23–28.
8. Landi, B. J.; Ganter, M. J.; Schauerman, C. M.; Cress, C. D.; Raffaelle, R. P. Lithium Ion Capacity of Single Wall Carbon Nanotube Paper Electrodes. *J. Phys. Chem. C* **2008**, *112*, 7509–7515.
9. Liu, F.; Song, S.; Xue, D.; Zhang, H. Folded Structured Graphene Paper for High Performance Electrode Materials. *Adv. Mater.* **2012**, *24*, 1089–1094.
10. Seng, K. H.; Liu, J.; Guo, Z. P.; Chen, Z. X.; Jia, D.; Liu, H. K. Free-Standing V_2O_5 Electrode for Flexible Lithium Ion Batteries. *Electrochem. Commun.* **2011**, *13*, 383–386.
11. Chou, S.-L.; Zhao, Y.; Wang, J.-Z.; Chen, Z.-X.; Liu, H.-K.; Dou, S.-X. Silicon/Single-Walled Carbon Nanotube Composite Paper as a Flexible Anode Material for Lithium Ion Batteries. *J. Phys. Chem. C* **2010**, *114*, 15862–15867.
12. Zhao, X.; Hayner, C. M.; Kung, M. C.; Kung, H. H. In-Plane Vacancy-Enabled High-Power Si–Graphene Composite Electrode for Lithium-Ion Batteries. *Adv. Energy Mater.* **2011**, *1*, 1079–1084.
13. Zhang, B.; Zheng, Q. B.; Huang, Z. D.; Oh, S. W.; Kim, J. K. SnO_2–Graphene–Carbon Nanotube Mixture for Anode Material with Improved Rate Capacities. *Carbon* **2011**, *49*, 4524–4534.
14. DiLeo, R. A.; Frisco, S.; Ganter, M. J.; Rogers, R. E.; Raffaelle, R. P.; Landi, B. J. Hybrid Germanium Nanoparticle–Single-Wall

Carbon Nanotube Free-Standing Anodes for Lithium Ion Batteries. *J. Phys. Chem. C* **2011**, *115*, 22609–22614.
15. Xie, S.; Li, W.; Pan, Z.; Chang, B.; Sun, L. Mechanical and Physical Properties on Carbon Nanotube. *J. Phys. Chem. Solids* **2000**, *61*, 1153–1158.
16. Dikin, D. A.; Stankovich, S.; Zimney, E. J.; Piner, R. D.; Dommett, G. H. B.; Evmenenko, G.; Nguyen, S. T.; Ruoff, R. S. Preparation and Characterization of Graphene Oxide Paper. *Nature* **2007**, *448*, 457–460.
17. Landi, B. J.; Ganter, M. J.; Cress, C. D.; DiLeo, R. A.; Raffaelle, R. P. Carbon Nanotubes for Lithium Ion Batteries. *Energy Environ. Sci.* **2009**, *2*, 638–654.
18. Ji, L.; Zhang, X. Fabrication of Porous Carbon Nanofibers and Their Application as Anode Materials for Rechargeable Lithium-Ion Batteries. *Nanotechnology* **2009**, *20*, 155705.
19. Ji, L.; Zhang, X. Fabrication of Porous Carbon/Si Composite Nanofibers as High-Capacity Battery Electrodes. *Electrochem. Commun.* **2009**, *11*, 1146–1149.
20. Lee, B.-S.; Park, K.-M.; Yu, W.-R.; Youk, J. An Effective Method for Manufacturing Hollow Carbon Nanofibers and Microstructural Analysis. *Macromol. Res.* **2012**, *20*, 605–613.
21. Lee, B.-S.; Son, S.-B.; Park, K.-M.; Lee, G.; Oh, K. H.; Lee, S.-H.; Yu, W.-R. Effect of Pores in Hollow Carbon Nanofibers on Their Negative Electrode Properties for a Lithium Rechargeable Battery. *ACS Appl. Mater. Interfaces* **2012**, *4*, 6702–6710.
22. Lee, B.-S.; Son, S.-B.; Park, K.-M.; Seo, J.-H.; Lee, S.-H.; Choi, I.-S.; Oh, K.-H.; Yu, W.-R. Fabrication of Si Core/C Shell Nanofibers and Their Electrochemical Performances as a Lithium-Ion Battery Anode. *J. Power Sources* **2012**, *206*, 267–273.
23. Lee, B.-S.; Son, S.-B.; Park, K.-M.; Yu, W.-R.; Oh, K.-H.; Lee, S.-H. Anodic Properties of Hollow Carbon Nanofibers for Li-Ion Battery. *J. Power Sources* **2012**, *199*, 53–60.
24. Lee, B.-S.; Son, S.-B.; Seo, J.-H.; Park, K.-M.; Lee, G.; Lee, S.-H.; Oh, K. H.; Ahn, J.-P.; Yu, W.-R. Facile Conductive Bridges Formed between Silicon Nanoparticles inside Hollow Carbon Nanofibers. *Nanoscale* **2013**, *5*, 4790–4796.
25. Zussman, E.; Chen, X.; Ding, W.; Calabri, L.; Dikin, D. A.; Quintana, J. P.; Ruoff, R. S. Mechanical and Structural Characterization of Electrospun PAN-Derived Carbon Nanofibers. *Carbon* **2005**, *43*, 2175–2185.
26. Arshad, S. N.; Naraghi, M.; Chasiotis, I. Strong Carbon Nanofibers from Electrospun Polyacrylonitrile. *Carbon* **2011**, *49*, 1710–1719.
27. Yang, Z.-h.; Wu, H.-q. Electrochemical Intercalation of Lithium into Carbon Nanotubes. *Solid State Ionics* **2001**, *143*, 173–180.
28. Lahiri, I.; Oh, S.-W.; Hwang, J. Y.; Cho, S.; Sun, Y.-K.; Banerjee, R.; Choi, W. High Capacity and Excellent Stability of Lithium Ion Battery Anode Using Interface-Controlled Binder-Free Multiwall Carbon Nanotubes Grown on Copper. *ACS Nano* **2010**, *4*, 3440–3446.
29. Vratsanos, L. A.; Farris, R. J. A Predictive Model for the Mechanical Behavior of Particulate Composites. Part I: Model Derivation. *Polym. Eng. Sci.* **1993**, *33*, 1458–1465.
30. Wang, Q.; Li, H.; Chen, L.; Huang, X.; Zhong, D.; Wang, E. Investigation of Lithium Storage in Bamboo-like CNTs by HRTEM. *J. Electrochem. Soc.* **2003**, *150*, A1281–A1286.
31. Hwang, H.; Kim, M. G.; Cho, J. Li Reaction Behavior of GaP Nanoparticles Prepared by a Sodium Naphthalenide Reduction Method. *J. Phys. Chem. C* **2007**, *111*, 1186–1193.
32. Kambe, N.; Dresselhaus, M. S.; Dresselhaus, G.; Basu, S.; McGhie, A. R.; Fischer, J. E. Intercalate Ordering in First Stage Graphite-Lithium. *Mater. Sci. Eng.* **1979**, *40*, 1–4.
33. Pastor, G. M.; Dorantes-Dávila, J.; Bennemann, K. H. A Theory for the Size and Structural Dependence of the Ionization and Cohesive Energy of Transition-Metal Clusters. *Chem. Phys. Lett.* **1988**, *148*, 459–464.
34. Krishnan, R.; Lu, T.-M.; Koratkar, N. Functionally Strain-Graded Nanoscoops for High Power Li-Ion Battery Anodes. *Nano Lett.* **2010**, *11*, 377–384.
35. Koo, M.; Park, K.-I.; Lee, S. H.; Suh, M.; Jeon, D. Y.; Choi, J. W.; Kang, K.; Lee, K. J. Bendable Inorganic Thin-Film Battery for Fully Flexible Electronic Systems. *Nano Lett.* **2012**, *12*, 4810–4816.
36. Hu, L.; Pasta, M.; Mantia, F. L.; Cui, L.; Jeong, S.; Deshazer, H. D.; Choi, J. W.; Han, S. M.; Cui, Y. Stretchable, Porous, and Conductive Energy Textiles. *Nano Lett.* **2010**, *10*, 708–714.